Chapter 6

Meteorology and modelling

Measurements tell us what the concentrations are (or have been) at a particular location. They cannot tell us what the concentration is going to be in the future, or what it is now at locations where no measurements are being made. Air pollution models help us to understand the way air pollutants behave in the environment. In principle, a perfect model would enable the spatial and temporal variations in pollutant concentration to be predicted to sufficient accuracy for all practical purposes, and would make measurements unnecessary. We are a very long way from this ideal. Also, it should be remembered that a model is no use unless it has been validated to show that it works, so that the process of model development goes hand in hand with developments in measurement. There are many reasons for using models, such as working out which sources are responsible for what proportion of concentration at any receptor; estimating population exposure on a higher spatial or temporal resolution than is practicable by measurement; targeting emission reductions on the highest contributors; predicting concentration changes over time.

There are four main families of model:

- Dispersion models, which are based on a detailed understanding of physical, chemical and fluid dynamical processes in the atmosphere. They enable the concentration at any place and time to be predicted if the emissions and other controlling parameters are known;
- Receptor models, which are based on the relationships between a data set of measured concentrations at the receptor and a data set of emissions that might affect those concentrations;
- Stochastic models, which are based on semi-empirical mathematical relationships between the pollutant concentrations and any factors that might affect them, regardless of the atmospheric physical processes;
- Compartment or box models, in which inputs to, and outputs from, a defined volume of the atmosphere are used to calculate the mean concentration within that volume.

All modelling and validation need some understanding of relevant meteorology, so we will cover that before looking at the models themselves.

6.1 METEOROLOGICAL FACTORS

The main meteorological factors that affect dispersion are wind direction, windspeed and atmospheric turbulence (which is closely linked with the concept of stability).

6.1.1 Wind direction

Wind direction is conventionally specified as the direction from which the wind is blowing, because we have been more interested in what the wind has collected before it reaches us than in where it will go afterwards. Wind direction is commonly identified with one of 16 (or sometimes 32) points of the compass (e.g. a south westerly wind is a wind blowing from the south-west), or more scientifically as an angle in degrees clockwise from north (so the south-west wind will be blowing from between 213.75° and 236.25°). What is spoken of colloquially as the wind direction is rarely constant in either the short or long term. The average value over periods of between one and a few hours is determined by meteorology – the passage of a frontal system, or the diurnal cycle of sea breezes near a coast, for example. This medium-term average value of wind direction is of fundamental importance in determining the area of ground that can be exposed to the emission from a particular source. Short-term variations (between seconds and minutes), due to turbulence, are superimposed on this medium-term average – they can be seen on a flag or wind-vane. As well as these short-term horizontal variations, there are also short-term variations in the vertical component of the wind that affect turbulent dispersion. The magnitudes of both horizontal and vertical variations are influenced by the atmospheric stability, which in turn depends on the balance between the adiabatic lapse rate and the environmental lapse rate. These concepts are described in Section 6.1.3.

6.1.2 Windspeed

Windspeed is measured in m s^{-1} or knots (one knot is one nautical mile per hour; one nautical mile is 6080 feet, or 1.15 statute miles). Although the use of SI units is encouraged in all scientific work, some professions have stuck with earlier systems. Thus mariners, pilots and meteorologists are all comfortable with knots. Mariners also use the Beaufort Scale, which relates windspeed to its effects on the sea.

Windspeed is important for atmospheric dispersion in three distinct ways. First, any emission is diluted by a factor proportional to the windspeed past the source. Second, mechanical turbulence, which increases mixing and dilution, is created by the wind. Third, a buoyant source (hot or cold) is 'bent over' more at higher windspeeds, keeping it closer to its release height. Friction with the ground reduces the windspeed near the surface, so that the speed at the top of an industrial chimney (such as that of a power station, which might be 200 m tall)

Table 6.1 Variation of the windspeed exponent *p* with stability category

Pasquill stability Class	*Exponent p for rough terrain*	*Exponent p for smooth terrain*
A – the most unstable	0.15	0.07
B	0.15	0.07
C	0.20	0.10
D	0.25	0.15
E	0.40	0.35
F – the most stable	0.60	0.55

will be substantially greater than at the bottom. The change with height can be approximated by a power law such as

$$u(z) = u_0 \, (z/z_0)^{\mathrm{p}} \tag{6.1}$$

where $u(z)$ is the windspeed at height z, u_0 is the windspeed measured by an anemometer at height z_0, p is an exponent that varies with atmospheric stability.

Table 6.1 gives the values of the exponent p appropriate to the Pasquill stability categories which are described in 6.1.3.5. This supports the intuitive idea that the best-mixed air (Class A) has the smallest variation of speed with height.

6.1.3 Atmospheric stability

6.1.3.1 Dry adiabatic lapse rate

Atmospheric pressure decreases exponentially with height. Hence, as an air parcel moves up (or down) in the atmosphere, it must expand (compress) and cool (warm). For a dry atmosphere (containing water vapour, but not liquid water droplets) the rate of decrease of temperature with height caused by this type of displacement is called the dry adiabatic lapse rate (Γ, or DALR). Adiabatic simply means that the air parcel's total energy content is conserved during the displacement, not exchanged with the surrounding air. The value of Γ is fixed by physical constants, and can be calculated from

$$\Gamma = g/c_{\mathrm{p}}$$

where g is the acceleration due to gravity $= 9.81$ m s^{-2} and c_{p} is the specific heat of air at constant pressure $= 1010$ J kg^{-1} K^{-1}.

Hence $\Gamma = 9.8$ °C km^{-1}. This value applies to sufficient accuracy in the lower 20 km of the atmosphere. Above that height, changes in the molecular

composition (which affect the molar mass) and in g (due to increasing distance from the centre of the Earth) start to affect the value. This is the reason for the steady decrease in temperature with height – up mountains, for example.

6.1.3.2 Saturated adiabatic lapse rate

If the air temperature falls below the water vapour dew point while the parcel is being lifted, then the excess water vapour will start to condense. This will release latent heat of vaporisation which will reduce the rate of cooling. Conversely, if a descending parcel contains liquid water droplets, then the process is reversed – the droplets evaporate as the parcel warms, extracting sensible heat from the air and reducing the rate of warming.

The variation of temperature with height when there is liquid water present is known as the saturated adiabatic lapse rate (SALR), or Γ_{sat}.

$$\Gamma_{sat} = \frac{dT}{dz} = \frac{-g}{c_p}\left\{\frac{1}{1 + (L/c_p)(dq_s/dT)}\right\} \tag{6.2}$$

where L is the latent heat of evaporation of water, q_s is the saturation mixing ratio (kg water/kg air).

Since the saturated vapour pressure of water depends on both the temperature and pressure, the SALR is also variable (Table 6.2). The minimum values are found for surface pressures and the warmest temperatures. Since the air also has to be saturated, this is more likely to be in the tropics than above the Sahara. Maximum values are found where the air is very cold, because then the water vapour content is low. The average lapse rate over the Earth is about 6.5 °C km^{-1}.

6.1.3.3 Atmospheric stability and temperature profile

The adiabatic lapse rates describe the temperature changes expected in a parcel of air when it is displaced vertically. This is not usually the same as the vertical

Table 6.2 Variation of saturated lapse rate (°C km^{-1}) with temperature and pressure

Pressure/mb	*Temperature*/°C				
	−40	−20	0	20	40
1000	9.5	8.6	6.4	4.3	3.0
800	9.4	8.3	6.0	3.9	
600	9.3	7.9	5.4		
400	9.1	7.3			
200	8.6				

temperature profile of the air, as would be measured, for example, by recording the temperature transmitted by a sounding balloon as it rose through the atmosphere. This environmental lapse rate (ELR) is the vertical variation, or profile, of air temperature with height that exists at any particular time and place. It may be equal to the adiabatic lapse rate over at least part of the height range of interest (up to, say, 1 km for pollutant dispersion), but it may be substantially different. The local balance between the two lapse rates gives an insight into the concept known as stability.

First, consider the different physical situations shown in Figure 6.1. In Figure 6.1(a), a marble is at rest in a bowl. Any small displacement of the marble results in a restoring force – a force that moves the marble back towards its initial position. Such a system is said to be stable. In Figure 6.1(b), the marble is on a flat surface. No force in any direction is generated by a displacement, and the system is described as neutral. Finally, in Figure 6.1(c), the marble is poised on the top of the upturned bowl. Now any displacement results in a force away from the initial position, and the system is unstable.

These ideas can be applied to air parcels in the atmosphere. Consider, for example, the different situations shown in Figure 6.2(a–c). In each Figure, the prevailing ELR is shown, and the DALR is given for comparison. A parcel of air that starts at A in Figure 6.2(a) and moves upward will cool at the DALR, reaching a lower temperature at B. However, the air around the parcel at the same height will be at C on the ELR. The parcel has become cooler and denser than its surroundings and will tend to sink back towards its starting height. If its initial displacement is downward, it will become warmer and less dense than its surroundings and tend to rise back up. The ELR is therefore stable, because small disturbances are damped out. In Figure 6.2(b), a rising parcel will again cool at the DALR. Since this is equal to the ELR, the parcel will be in air of the same temperature and density after displacement. The ELR is therefore neutral, because vertical motions are neither accelerated nor damped. Examination of vertical displacements for Figure 6.2(c) shows that they are accelerated, and that such an ELR is unstable.

If we look at the forces acting on a parcel displaced upwards in a stable atmosphere, an equation of motion can be written for which the solution is an

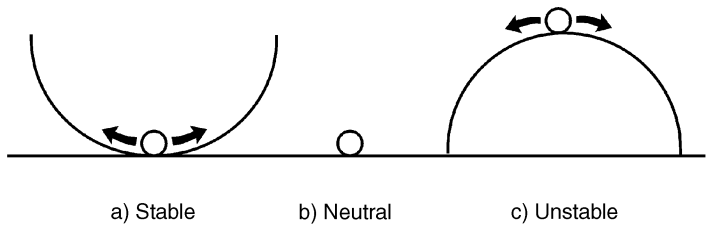

Figure 6.1 Stable, neutral and unstable systems.

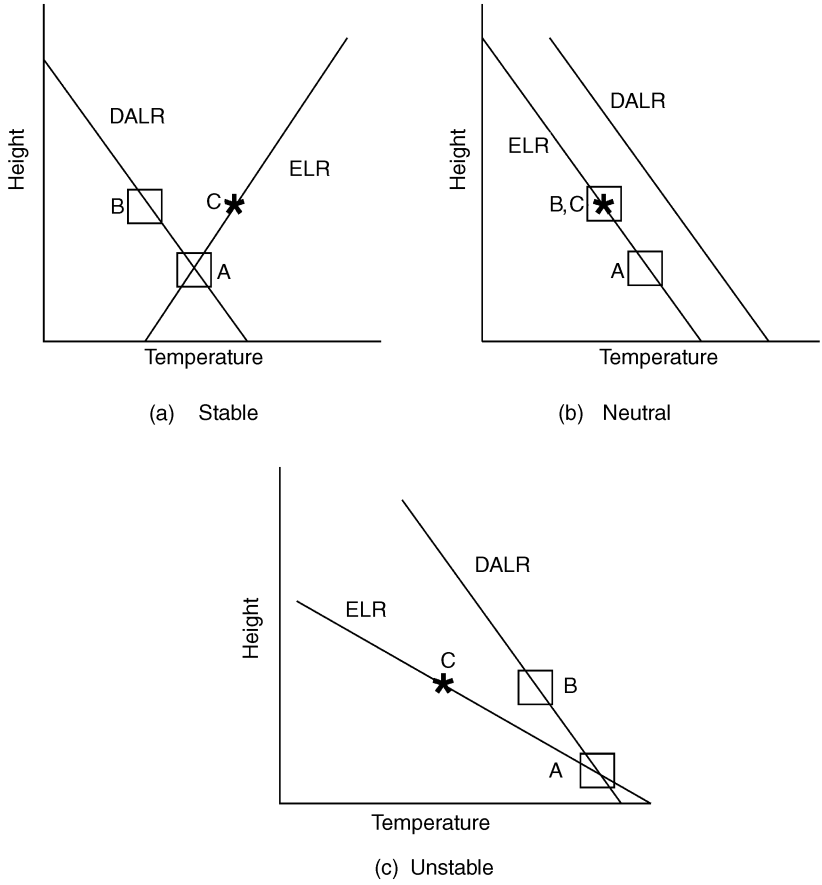

Figure 6.2 (a) Stable; (b) neutral; and (c) unstable Environmental lapse rates.

oscillation about the starting height. That is, the parcel experiences a restoring force that accelerates it back towards its original position. Since by then it is moving, it overshoots downwards, and a restoring force accelerates it upwards again, and so on. The frequency of this oscillation, which is called the buoyancy frequency, corresponds to a natural period of a few minutes in the lower atmosphere.

In practice, real temperature profiles in the atmosphere often consist of a mixture of different ELRs, so that vertical dispersion will be different at different heights. Consider the Environmental Lapse Rate shown in Figure 6.3. Between A and B, strong solar heating of the ground has warmed the lowest layers of air; the middle layer BC is close to DALR, while the layer CD is showing an increase of temperature with height (this is known as an inversion of the temperature profile).

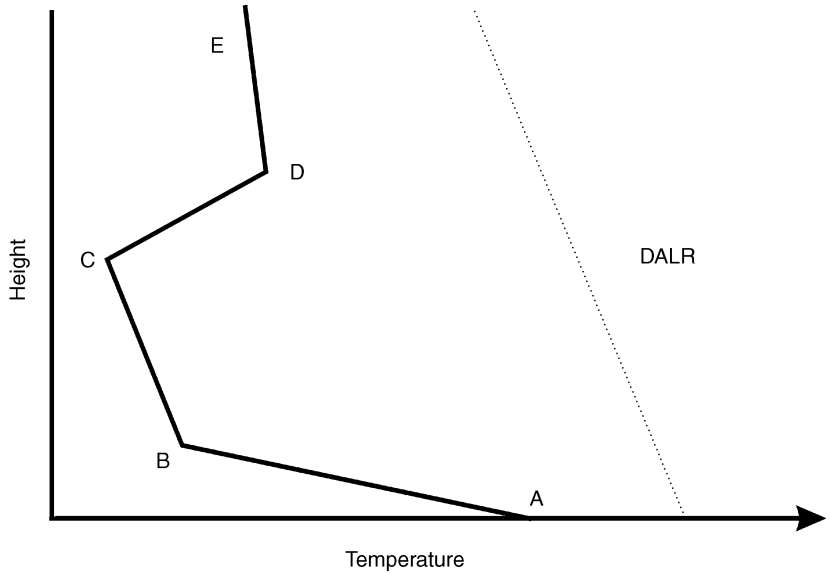

Figure 6.3 An atmospheric temperature profile involving a range of stabilities.

This profile will be very unstable (strong dispersion) in AB, close to neutral in BC, and very stable (poor dispersion) in CD. When a persistent anticyclonic high pressure region is present, there is often an area in the centre where high-level air is sinking. The sinking raises the temperature, generating an elevated inversion which may act as a lid to vertical plume dispersion and increase ground-level pollutant concentrations. Since the pressure gradients and hence windspeeds are low under these meteorological conditions, a serious pollutant episode may result.

We saw in Section 6.1.3.2 that the lapse rate for saturated air is lower than for dry air. Hence the same air mass may be stable or unstable, depending on whether it is saturated or not. As an unsaturated air parcel starts to rise, it will cool at the dry lapse rate of 9.8 °C km^{-1}. If the ELR is, say 8 °C km^{-1}, then the movement is stable. But if the upward movement cools the air enough to cause condensation of water vapour, then the lapse rate will fall to the saturated value of, say 7 °C km^{-1}, and the displacement is now unstable. This is called conditional instability. The condition is not rare – since the average global lapse rate of 6.5 °C falls between the dry adiabatic rate and the average moist lapse rate of 6 °C, conditional instability is the norm. Furthermore, a humidity gradient can change the stability. This is most often seen in the warm atmosphere near the surface above the tropical ocean. The sea surface evaporates water into the air. The molar mass of water is 18 compared with 29 for the air, so the air density decreases and promotes instability.

6.1.3.4 Potential temperature

A useful additional concept is that of potential temperature, θ. The DALR shows a steady reduction of temperature with height, and it is not obvious at first glance whether a particular rate of reduction is greater than or less than the DALR. This divergence is important for the assessment of atmospheric stability and pollutant dispersion, as we have seen. We can define the potential temperature of an air parcel at any pressure (i.e. height) as the temperature that it would have if the parcel were moved adiabatically to a standard or reference pressure. This reference pressure is normally taken to be 100 kPa, which is very close to the standard global average atmospheric pressure at sea level of 101.325 kPa. The potential temperature, then, is the temperature that the parcel would have if it was moved down to sea level adiabatically. By definition, θ is constant for an air parcel that is moved upwards adiabatically from sea level. An actual temperature profile such as that in Figure 6.4 is transformed into a potential temperature profile, where parts with neutral stability are vertical; in stable atmospheres θ increases with height, while in unstable atmospheres it decreases with height.

6.1.3.5 Pasquill stability classes

The general effect of environmental variables on stability can be summarised as follows:

- On cloud-free days, solar radiation will warm the ground during the day, making the lowest air layers unstable.
- On cloud-free nights, net upwards longwave thermal radiation cools the ground, making the lowest air layers stable, and creating a ground-level inversion.
- As windspeed rises, vigorous vertical exchange tends to generate a neutral ELR equal to the DALR.
- As cloud cover increases, daytime heating and nighttime cooling of the ground are both reduced, again making the ELR closer to the DALR.
- A persistent high pressure region has a downward air movement at the centre, which often creates an elevated inversion and traps pollutants near the ground. This is known as ‘anticyclonic gloom’.

The influence of solar radiation and windspeed on stability led Pasquill to identify stability classes on a scale from A (very unstable) to G (very stable), and to relate them to the meteorology in the simple way shown in Table 6.3.

First, look at the stability classes during the daytime. When the sun is strong and the winds light, we would expect maximum ground heating, raising the temperature of the lowest layers of air and creating unstable conditions. With less sunshine, this effect is reduced and the instability is less marked. As the windspeed increases, vertical mechanical mixing starts to override the buoyancy effects, and frequent exchanges of air parcels at DALR generate a neutral ELR (class D). At night, net radiation losses and ground cooling are most marked under clear

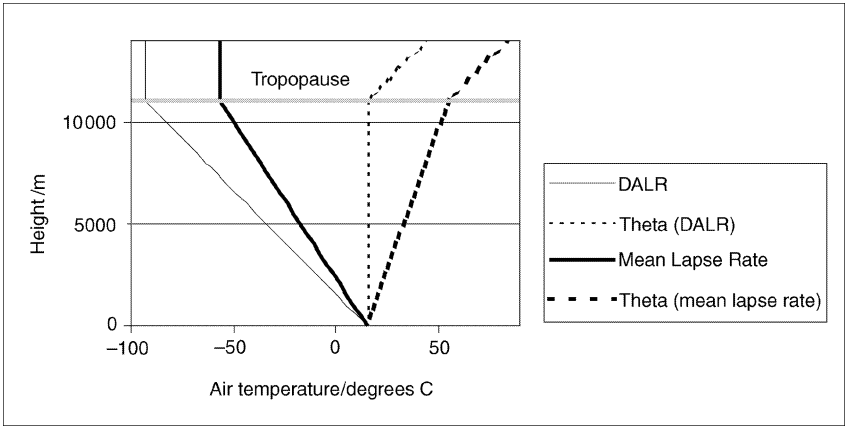

Figure 6.4 Actual and potential temperature profiles.

Table 6.3 Dependence of stability on meteorological parameters

Surface windspeed ms^{-1}	*Day time sun (flux density in* W m^{-2}*)*			*Night time (cloud amount in oktas)*		
	Strong (>590)	*Moderate* (300–590)	*Weak* (<290)	8	4–7	0–3
<2	A	A–B	B	D	G	G
2–3	A–B	B	C	D	E	F
3–5	B	B–C	C	D	D	E
5–6	C	C–D	D	D	D	D
>6	C	D	D	D	D	D

skies. As the ground cools, the lowest air layers become stable (class G). The cloudier or the windier it becomes, the more probable class D becomes again.

Occurrence of Pasquill classes

Table 6.4 shows the average occurrence of different stability classes in the UK. As would be expected, our temperate maritime climate gives us high average windspeeds and cloud cover, so that categories C and D are the most likely. The very high values for ELR given here, equivalent to up to 40 °C km^{-1}, can only be sustained within the lowest few metres of the atmosphere.

6.1.3.6 Other stability estimators

The Pasquill scheme described in Section 6.1.2 is semi-quantitative, in that it ascribes categories to ranges of the driving variables wind speed and solar radiation, but does

Table 6.4 Occurrence of different stability classes in the UK

Stability class	*Occurrence in UK/%*	*ELR* °C (100 m)$^{-1}$	*u at* 10 m ms^{-1}	*Weather*
A: Very unstable	1	<-1.9	1.0–2.5	Very sunny
B: Moderately unstable	5	-1.9–-1.7	1.0–5.0	Sunny
C: Slightly unstable	15	-1.7–-1.5	2.0–6.0	Part cloud (day)
D: Neutral	65	-1.5–-0.5	2.0–>10.0	Overcast
E: Stable	6	-0.5– $+1.5$	2.0–5.0	Part cloud (night)
F: Very stable	6	$+1.5$– $+4.0$	2.0–3.0	Clear night
G: Even more stable than F	2		Calm	

not involve a formula with explicit values. There are two more quantitative parameters in common use – the Richardson Number and the Monin–Obukhov length.

The Richardson Number

The Richardson Number Ri is calculated from gradients of temperature and windspeed

$$\mathrm{Ri} = \frac{\dfrac{g}{T}\dfrac{\partial T}{\partial z}}{\left(\dfrac{\partial u}{\partial z}\right)^2}$$

where T is the absolute temperature.

The Richardson Number is dimensionless. We can see by inspection that if temperature increases strongly with height, which is the stable condition that we have discussed in Section 6.1.3.3, then Ri will tend to be large and positive. If T decreases with height at the adiabatic lapse rate, Ri will be negative. If there is a large gradient of windspeed with height, Ri will be small.

$\mathrm{Ri} < -1$	free convection
$-1 < \mathrm{Ri} < -0.01$	unstable mixed convection
$-0.01 < \mathrm{Ri} < +0.01$	forced convection
$+0.01 < \mathrm{Ri} < +0.1$	damped forced convection
$\mathrm{Ri} > 0.1$	increasingly stable

The Richardson Number is mainly used by meteorologists to describe events in the free atmosphere, rather than by air pollution scientists discussing dispersion closer to the ground.

The Monin–Obukhov Length

The Monin–Obukhov Length, L is a function of heat and momentum fluxes.

$$L = -\frac{\rho c_p T u_*^3}{kgC}$$

where T is the absolute temperature and C is the vertical sensible heat flux.

The formula for L recognises the two contrasting processes that drive atmospheric turbulence and dispersion. Mechanical turbulence is generated by wind blowing over surface roughness elements. It is therefore strongest at the surface, and reduces upward depending on the stability. Convective turbulence is generated by heat flux from the surface, and will increase upwards in unstable conditions but be damped out in stable conditions (Table 6.5). The result has units of metres, and represents the scale of the turbulence. Since C may be positive (up) or negative (down), L may be positive or negative. When conditions are unstable or convective, L is negative, and the magnitude indicates the height above which convective turbulence outweighs mechanical turbulence. When conditions are stable, L is positive, and indicates the height above which vertical turbulence is inhibited by stable stratification. In practice, values range between infinity (in neutral conditions when C is zero) and -100 m. Atmospheric stability is related to the ratio h/L, where h is the depth of the boundary layer. L is increasingly being used in dispersion models as a more sophisticated estimator of turbulence than the Pasquill category.

For practical use in the lowest few hundred metres of the atmosphere, we can write

$$L = \left(\frac{\rho c_p T}{kg}\right)\frac{u_*^3}{C} = \text{const.}\frac{u_*^3}{C}. \tag{6.3}$$

Note that although this expression does not look like a length at first sight, the dimensions do confirm that it is
i.e.

$(\text{kg m}^{-3})(\text{J kg}^{-1}\text{ K}^{-1})(\text{K})(\text{m s}^{-1})^3/(\text{m s}^{-2})(\text{W m}^{-2})$ has dimensions of length and units of metres.

Table 6.5 Stability as a function of L and h

Stability	*Range of h/L*
Stable	$h/L \geq 1$
Neutral	$-0.3 \leq h/L < 1$
Convective	$h/L < -0.3$

The values of ρ, c_p, T, k and g are then taken as constant.
With

$\rho = 1.2$ kg m^{-3}
$c_p = 1010$ J kg^{-1} K^{-1}
$T = 288$ K (15 °C)
$k = 0.41$
$g = 9.81$ m s^{-2},

we have $L = 8.7 \times 10^4 \, u_*^3/C$

Other stability estimators have been used, such as the standard deviation of the fluctuations in the horizontal wind direction, and the ratio of the windspeeds at two heights. Comparisons of the predictions made by different estimators from the same data set have shown that the Monin–Obukhov length method correlates best with the Pasquill classes.

Boundary layer height

The Monin–Obukhov formulation can also be used to estimate the height of the boundary layer in stable-to-neutral conditions, from

$$\frac{h}{L} = \frac{0.3u_*/|f|L}{1+1.9h/L}$$

The situation in unstable conditions is more complex, because the boundary layer grows from an initial value of zero when the surface heat flux becomes positive, at a rate governed by the surface heat flux, the temperature jump across the top of the layer, and the friction velocity (Table 6.6).

Table 6.6 Relationships between stability estimators

Windspeed u/m s^{-1}	*Pasquill category*	*Boundary layer height* h/m	*Monin–Obukhov Length*/m	*h/L*
1	A	1300	−2	−650
2	B	900	−10	−90
5	C	850	−100	−8.5
5	D	800	∞	0
3	E	400	100	4
2	F	100	20	5
1	G	100	5	20

6.1.4 Meteorological data

In the UK the main provider of meteorological data is the Meteorological Office. Typically a user, such as a Local Authority, will need to use a commercial dispersion model to calculate ground-level concentrations of a pollutant from a particular source. If this is done hour-by-hour for one year, then 8760 sets of meteorological data will be needed. Each set will include values of wind speed, wind direction, boundary layer height and an atmospheric stability criterion such as Pasquill class or Monin–Obukhov length scale. Wind speed and direction may be measured locally, but the other parameters are derived from other values and different methods are in use. Trinity Consultants are the main provider of nation-wide data in the US, and this company also supplies compilations of UK data in the UK.

6.2 DISPERSION MODELS

The qualitative aspect of dispersion theory is to describe the fate of an emission to atmosphere from a point, area or line source. Quantitatively, dispersion theory provides a means of estimating the concentration of a substance in the atmosphere, given specific information about meteorological factors and the geometry and strength of the source. Dispersion models include:

- Eulerian models, which numerically solve the atmospheric diffusion equation. Eulerian models work on the measurement of the properties of the atmosphere as it moves past a fixed point. A windvane or cup anemometer are Eulerian sensors.
- Gaussian models, which are built on the Gaussian (normal) probability distribution of wind vector (and hence pollutant concentration) fluctuations. Strictly these are a subset of Eulerian models but are usually treated as a group in their own right.
- Lagrangian models, which treat processes in a moving airmass, or represent the processes by the dispersion of fictitious particles. Tracking a neutral-density balloon as it moves downwind is a Lagrangian measurement.

Dispersion is essentially due to turbulence, and turbulence occurs with a great range of length scales in the atmosphere. Hence there are further families of model depending on the length (or time) scale of interest:

- Macro scale (~1000 km, or days). Atmospheric flow is driven by synoptic phenomena such as high/low pressure areas. For example, the long range transport of air pollution from Central Europe to the UK or from the UK to Scandinavia.
- Meso scale (10s–100s of km, or hours). Air movement is synoptically driven, but modified by local effects such as surface roughness and obstacles. For

example, the dispersion of emissions from a power station chimney over the surrounding countryside.
- Microscale (<1 km, or minutes). Air flow depends mainly on local features. For example, urban flows in the labyrinth of street canyons.

6.3 GAUSSIAN DISPERSION THEORY

Eulerian models are based on the concept of a fixed reference point, past which the air flows. Lagrangian models, in contrast, are based on the concept of a reference point that travels with the mean flow. In the commonly-used Gaussian method, the simplest realisation of this idea is to think of an instantaneous release of a pollutant from a point source. This 'puff' moves downwind along the average wind direction. As it does so it expands in volume, incorporating dilution air from around it and reducing its concentration. The puff also experiences small random movements, caused by turbulence, away from the mean direction. A continuous emission is then described as an infinitely rapid series of small individual puffs. Gaussian dispersion theory enables the concentration due to such a trajectory to be calculated at any location downwind.

We are now going to outline the system of equations that we need in order to predict what concentration of a substance will be found at any point in the atmosphere, if that substance is being released at a known rate from a source. We will show how the practical equations are related to physical processes in the atmosphere, but we will not derive the equations from first principles.

6.3.1 Coordinate system

First, we have to be able to describe the position of the place at which we wish to estimate concentration, relative both to the source and the ground. A standard Cartesian (x, y, z) coordinate system is used (Figure 6.5).

In this coordinate system:

the physical source (e.g. the base of a chimney) is located at the origin (0, 0, 0);
the x axis lies along the mean wind direction;
x is the distance downwind from the source;
y is the lateral distance from the mean wind direction;
z is the height above ground level;
h is the physical height of the chimney;
dh is the additional height by which the plume rises due to its buoyancy and/or momentum;
$H = h + dh$ is the effective height of the release;
$\overline{u}$ is the mean windspeed at plume height.

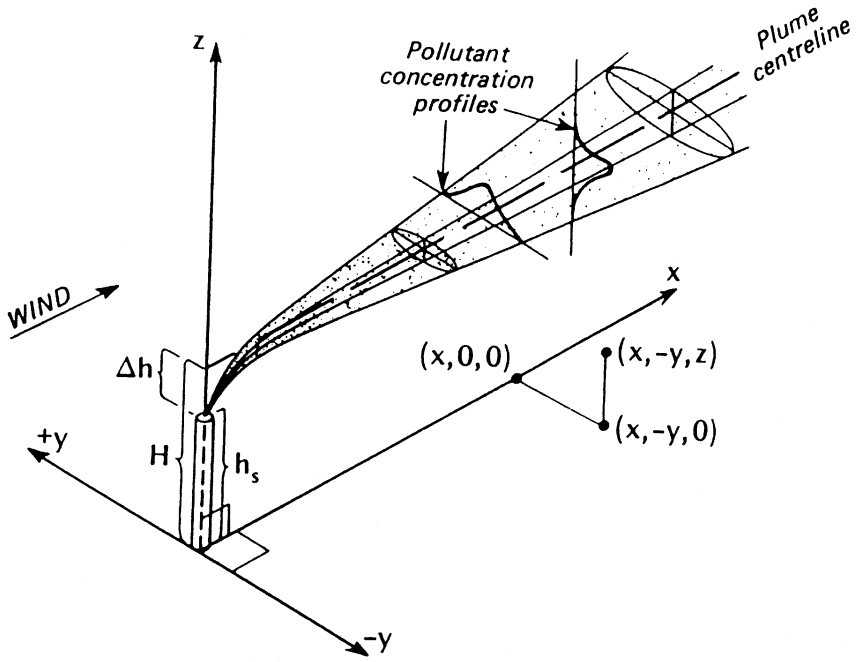

Figure 6.5 The Cartesian coordinate system used to specify dispersion geometry.

6.3.2 Fickian diffusion

The starting point for dispersion theory is to consider the diffusion of a cloud of material released into the atmosphere instantaneously from a point source. In one dimension, turbulent transfer in the atmosphere can be described by a Fickian equation of the form

$$\frac{d\,\overline{q}}{dt} = K\frac{\partial^2 \overline{q}}{\partial x^2}$$

where q is the concentration of material and K is the turbulent diffusivity. This equation has an analytical solution

$$\overline{q} = \frac{Q}{(4Kt)^{0.5}}\exp\left(\frac{-x^2}{4Kt}\right)$$

where Q is the source strength (e.g. in kg s^{-1}). The concentration is a maximum at the point of release, and decays away in both positive and negative directions following the Gaussian bell-shaped distribution (Figure 6.6). Hence the value of

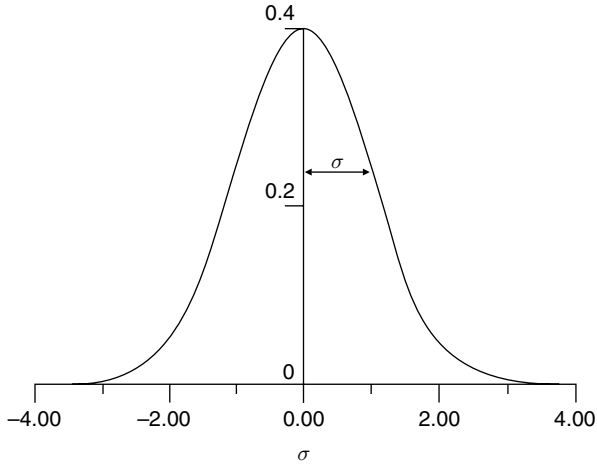

Figure 6.6 The standard Gaussian (normal) distribution, showing the physical significance of sigma.

σ at any distance from the source is a distance in metres which represents the lateral or vertical half 'width' of the plume.

Now imagine that this instantaneous point source of material is diffusing isotropically in three dimensions (puff model) and at the same time drifting away from the point of release at the average windspeed $\bar{u}$. The solution becomes

$$q(x, y, z, t) = \frac{Q}{(2\pi\sigma^2)^{3/2}} \exp\left(\frac{-r^2}{2\sigma^2}\right)$$

where σ is the standard deviation of the puff concentration at any time t, and $r^2 = (x - \bar{u}t)^2 + y^2 + z^2$.

6.3.3 The Gaussian plume equation

Following the analysis given for puff dispersion, emission from a continuous source can be considered as a continuous series of overlapping puffs, giving

$$q(x, y, z) = \frac{Q}{2\pi\bar{u}\sigma_y\sigma_z} \exp\frac{-y^2}{2\sigma_y^2} \exp\left\{\frac{-(z-H)^2}{2\sigma_z^2}\right\} \tag{6.4}$$

where σ_y and σ_z are the standard deviations in the y and z directions, respectively; and H is the total height of release. The first exponential term describes

lateral dispersion, and the second describes vertical dispersion. Equation 6.4 is the basic Gaussian dispersion equation which is at the heart of many air quality prediction models.

It is important to realise that σ_y and σ_z describe the width of the concentration distribution, not of the plume itself. This aspect is clarified in Figure 6.7. The plan view shows a snapshot of the plume at any one time as the plume wanders either side of the mean wind direction. The concentration within the plume itself is approximately uniform, as shown by the 'top hat' shape of the

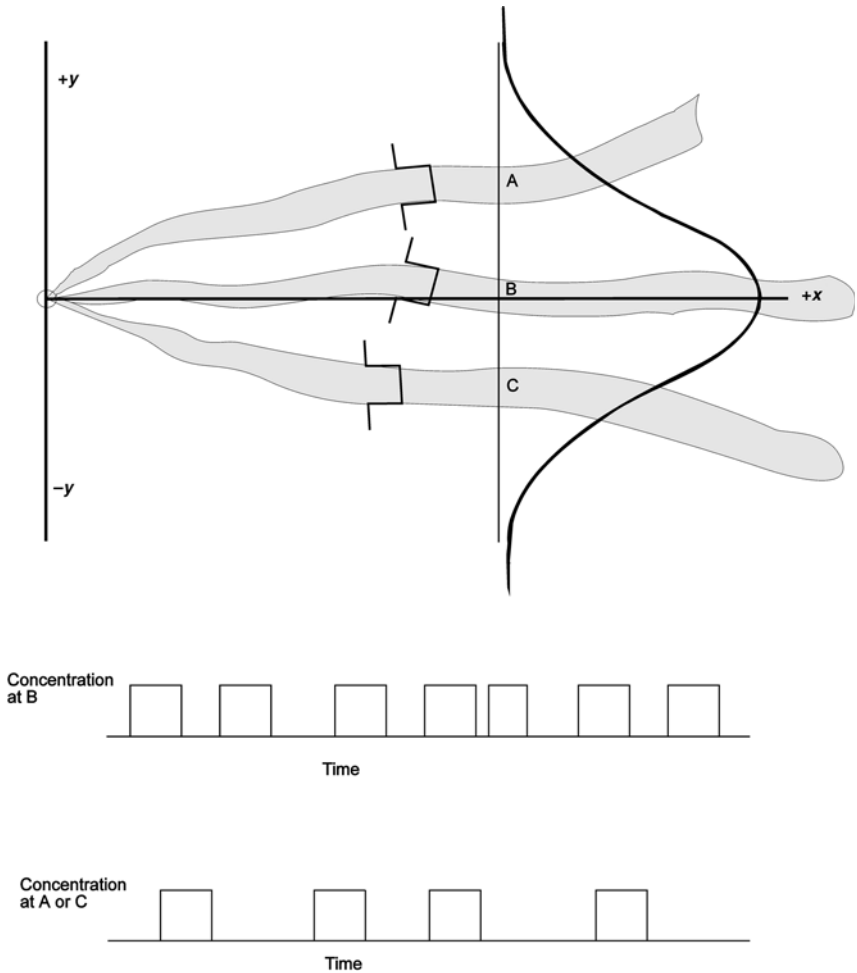

Figure 6.7 A plan view showing how the Gaussian distribution is formed from the differing frequency of exposure to the plume as it wanders about the mean wind direction.

distribution. The plume moves across to locations A and C only rarely – although the peak concentration may be high for a short time, the average is low because most of the time the plume is elsewhere. Point B is on the centre line of the plume along the mean wind direction. By definition, the plume spends a higher proportion of the time in this direction than any other, so the average concentration is highest. The frequency distribution of direction variations about the mean is Gaussian – hence the lateral Gaussian profile is built up. Similar variations in the vertical plane also give a Gaussian profile.

6.3.4 Assumptions of the Gaussian model

- Release and sampling times are long compared to the travel time from source to receptor. This means that the release is effectively steady state and that diffusion along the mean wind direction is negligible compared to advection (movement with the mean wind). Measurement time scales of hours rather than minutes are implied.
- The material is chemically stable and is not deposited to the ground. This means that gases must be unreactive, and particles must be <20 μm in diameter so that they do not sediment out. The equation of continuity will then apply – the integral of the concentration over all space at any time is equal to the total mass of material emitted. In practice, most gases are deposited to some extent; this can be allowed for by, for example, an additional exponential decay factor in the concentration with distance from the source.
- The lateral and vertical variations of the material concentration can both be described by Gaussian distributions, which are functions of x only.
- The windspeed is constant with height. This is never true in practice, as has already been seen. Windspeed variation with height can often be described by a logarithmic profile. More advanced versions of the Gaussian formulation divide the atmosphere up into layers, each layer having a specified set of characteristics such as windspeed and stability.
- The wind direction is constant with height. Again, this is rarely true. The most common form of the variation is the Ekman spiral, in which the direction tends towards the geostrophic (parallel with the isobars) as height increases, over the first few hundred metres.

6.3.5 Plume rise

Most plumes have either some exit velocity that carries them up into the air, or some degree of buoyancy due to temperature or density difference with the surrounding air, or both. Hence the effective plume height is likely to be different (usually, greater) than the physical height of the chimney. The dispersion equation

shows that concentration is a function of the square of the release height, and hence much research has been done into the dependence of plume rise on other factors.

In principle it is possible to solve the conservation equations for mass, momentum, enthalpy and amount of emitted material, and hence predict the trajectory of the plume and the rate of entrainment into it of surrounding air. A simplified, more empirical method has often been used which is less mathematically and computationally intensive, although increased computing power is making full solution more practical.

The standard theory assumes that a rising buoyant plume entrains ambient air at a rate proportional to both its cross-sectional area and its speed relative to the surrounding air. The driving force is expressed in terms of an initial buoyancy flux F_b, where

$$F_{\mathrm{b}} = w_0 R_0^2 \frac{g}{T_{\mathrm{p0}}} (T_{\mathrm{p0}} - T_{\mathrm{a0}})$$

with w_0 the initial plume speed, R_0 the inside stack radius, T_{p0} the initial plume temperature (K), and T_{a0} the ambient temperature at stack height. Hence the SI units of F_{b} are $\mathrm{m}^4\ \mathrm{s}^{-3}$.

Briggs solved the equations of motion for a bent-over plume in a neutral atmosphere to show that the height z at any distance x downwind was given by

$$z = \frac{C_1 \left(\frac{F_{\mathrm{b}}}{\pi} \right)^{\frac{1}{3}} x^{\frac{2}{3}}}{u} \left(1 + \frac{u\tau}{x} \right)^{\frac{1}{3}} = C_1 Br(F_{\mathrm{b}}, x, u)$$

where $Br(F_{\mathrm{b}}, x, u)$ is the 'Briggs variable'

and

$$\text{and } C_1 = \left(\frac{3}{2\beta^2} \right)^{\frac{1}{3}}, \text{ with plume radius } r = \beta z.$$

The most important value for use in dispersion calculations is the final plume rise *dh*. This has usually been found by fitting curves to observed data from a range of sources, and Briggs recommended the following relationships

Buoyant rise in unstable – neutral atmospheres

In Pasquill categories A–D, different equations are to be used depending on whether F_{b} is greater or less than 55 $\mathrm{m}^4\ \mathrm{s}^{-3}$.

$$\text{For } F_{\mathrm{b}} < 55 \text{ use } dh = 21\ \mathrm{F}^{0.75}/\mathrm{u}_h \tag{6.5}$$

For $F_b \geq 55$ use $dh = 39\ F^{0.6}/u_h$ (6.6)

where u_h is the windspeed at height h.

Buoyant rise in stable atmospheres

In a stable atmosphere, Briggs found that the most reliable expression for the final plume rise dh was given by

$$dh = 2.6\left(\frac{F_b}{uS}\right)^{1/3}$$

Here S, the ambient stability factor $= \frac{g}{T}\left(\frac{\partial T}{\partial z} + \Gamma\right)$, and is a function of atmospheric conditions only.

Clearly, these estimates of plume rise need quite detailed information about the properties of the source. If less is known about the source, dh can be estimated from

$$dh = \frac{515 P_T^{0.25}}{\overline{u}}$$

which gives the plume rise in metres when P_T is the thermal power of the chimney gases in MW – i.e. the product of mass flow rate, the specific heat of the flue gases and their temperature difference from that of the ambient air. For example, a large power station will have an electrical output at full load of 2000 MW, and a thermal output in the flue gases of about 280 MW. Hence a plume rise of 220 m would be expected in a windspeed of 10 m s^{-1}. The chimney height for such a power station in the UK is around 200 m, so plume rise contributes significantly to dispersion, especially since ground level concentrations are inversely proportional to the square of the effective source height.

6.3.6 The effect of vertical constraints

The simplest Gaussian solution (Eqn 6.4) assumes that the plume is free to expand in all directions without constraint. This may be true in practice during a limited period of time when an emission is moving away from an elevated source and has not yet moved close to the ground. For real sources, the pollutant cannot disperse in all directions without constraint. In the usual situation of an elevated source (chimney + plume) at some height above the ground, downward dispersion is always limited by the presence of the ground, while upward dispersion may be limited by an elevated inversion.

6.3.6.1 Reflection at the ground

Assuming that no pollutant is absorbed by the ground, any pollutant that reaches the ground is available for upward dispersion into the atmosphere again. This is accounted for theoretically by adding an 'image source', equal in magnitude to the actual source but located at (0, 0, −H), i.e. a distance 2*H* vertically below the actual source and distance *H beneath* the ground surface (Figure 6.8). Although this is a physically meaningless mathematical contrivance, it does the required job of effectively reflecting the plume away from the ground.

The dispersion equation therefore becomes

$$q(x, y, z) = \frac{Q}{2\pi\bar{u}\sigma_y\sigma_z} \exp\frac{-y^2}{2\sigma_y^2}\left\{\exp\frac{-(z-H)^2}{2\sigma_z^2} + \exp\frac{-(z+H)^2}{2\sigma_z^2}\right\} \quad (6.7)$$

where the second exponential term inside the curly brackets represents 'additional' material from the image source located at (0, 0, −H). This is shown as Image Source A on Figure 6.9.

6.3.6.2 Reflection at an inversion

Dispersion downwards will always be constrained by a physical surface such as water or vegetation. Dispersion upwards may also be constrained – not by a physical surface but by the temperature structure of the atmosphere itself. If there is an elevated inversion present, as was described in Figure 6.3, then this can act as a barrier to free upward dispersion. Buoyant air parcels penetrating into an elevated inversion from below will have buoyancy removed because the temperature of the surrounding air will increase with height while that of the parcel will decrease. The worst pollution episodes, such as those that occurred in London in

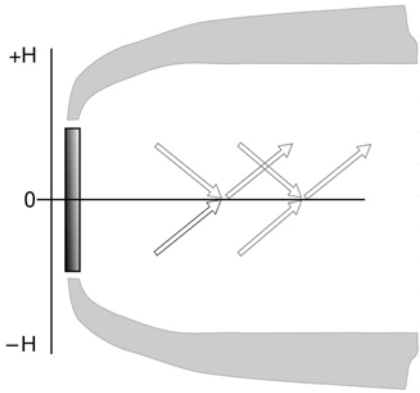

Figure 6.8 Side view to show how the image source allows for reflection of plume material at the ground.

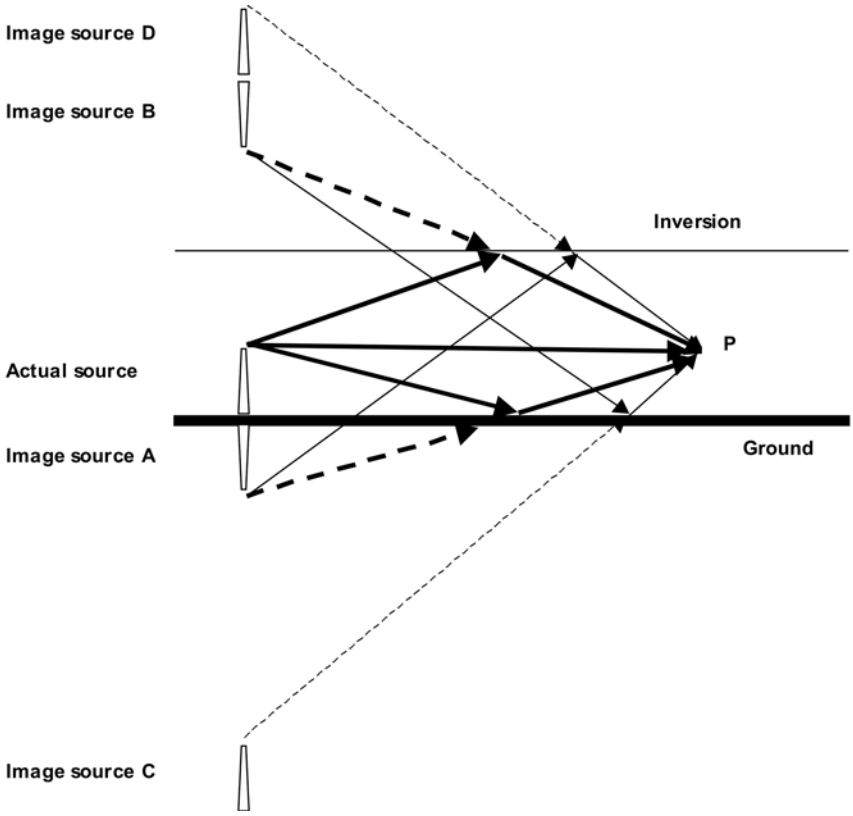

Figure 6.9 Schematic showing reflections of plume at ground and inversion.

1952 and 1991, are often associated with the presence of ground-level or low-altitude elevated inversions that trap ground-level emissions within a thin layer of the atmosphere. This is allowed for in the solution to the diffusion equation by the addition of further reflection terms, which are generated by an image source as far above the inversion as the actual source is below it (i.e. at a height of $(2H_{\mathrm{bl}} - H)$). Hence

$$q(x, y, z) = \frac{Q}{2\pi\bar{u}\sigma_y\sigma_z} \exp\frac{-y^2}{2\sigma_y^2}\left\{\exp\frac{-(z-H)^2}{2\sigma_z^2} + \exp\frac{-(z+H)^2}{2\sigma_z^2} + \exp\frac{-(z-2H_{\mathrm{bl}}+H)^2}{2\sigma_z^2} + \exp\frac{-(z+2H_{\mathrm{bl}}-H)^2}{2\sigma_z^2} + \exp\frac{-(z-2H_{\mathrm{bl}}-H)^2}{2\sigma_z^2}\right\} \quad (6.8)$$

where H_{bl} is the height of the inversion or the top of the boundary layer. In this equation, the first term in the curly brackets is the direct component, and the second is due to the image source discussed above. Figure 6.9 shows how these and the other components contribute to the concentration at any point P. The third exponential term in the curly brackets represents reflection of the source at the inversion (Image source B, Figure 6.9), the fourth term (Image source C) is reflection of Image source B at the ground, and the fifth (Image source D) is reflection of Image source A at the inversion.

Far enough downwind, the plume has expanded so far vertically that it fills the boundary layer completely. This occurs for $\sigma_z > H_{bl}$. After that it expands as a horizontal wedge, as though it had been released from a vertical line source the height of the boundary layer. The plume is well mixed throughout the boundary layer, so there is no z dependence and the concentration is given by

$$C(x, y) = \frac{Q}{\sqrt{2\pi}\sigma_y h U_{h/2}} \exp\left(\frac{-y^2}{2\sigma_y^2}\right) \tag{6.9}$$

The Gaussian formulation described above applies to stable and neutral boundary layers. There is increasing evidence that the distribution of vertical velocities, and hence of concentrations, is non-Gaussian (skewed) when the boundary layer is convective. The result of this skewness is that for elevated sources, the height within the plume at which the concentration is a maximum descends as the plume moves downwind, while the mean height of the plume rises.

6.3.7 Estimating stability

Figure 6.10 shows the idealised effect of the different ELRs on plume behaviour. Each diagram shows a temperature profile in the atmosphere, together with the expected plume behaviour. The most unstable conditions (a, Pasquill A) can result intermittently in very high concentrations of poorly-diluted plume close to the stack. This is called looping. Neutral conditions (b, Pasquill C–D) disperse the plume fairly equally in both the vertical and horizontal planes. This is referred to as coning. A strong inversion of the profile (c, Pasquill E–F) prevents the plume from mixing vertically, although it can still spread horizontally. If the plume is released above a ground-based inversion (d), then it is prevented from mixing down to the ground and ground-level concentrations are kept low. Conversely, if it is released below an elevated inversion (e) then it is prevented from dispersing upwards and ground-level concentrations are enhanced. In practice, complex ELR structures interact with stack and plume heights to create a much more variable picture.

The effect of stability on dispersion pattern can also be seen in Figure 6.11. Pasquill A generates the highest maximum concentration and the closest to the stack, although the narrow peak means that the integrated downwind concentration is low. As stability increases, the peak concentration decreases and moves downwind.

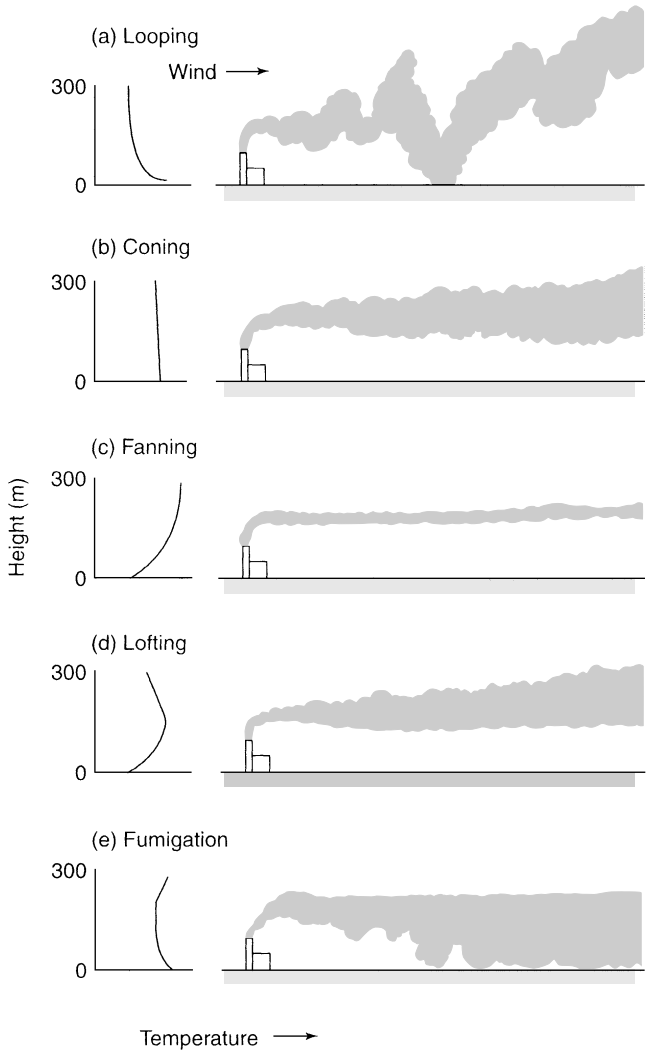

Figure 6.10 Effect of lapse rate on plume dispersion.
Source: Oke, T. R. (1987) *Boundary Layer Climates*, Methuen, London.

6.3.7.1 *Estimates of σ_y, σ_z*

Expressions for σ_y and σ_z have been derived in terms of the distance travelled by the plume downwind from the source under different Pasquill stability classes. They are available both as graphs and as empirical equations that are valid in the range 100 m $< x <$ 10 km. Figure 6.12(a) and (b) show the variations of standard

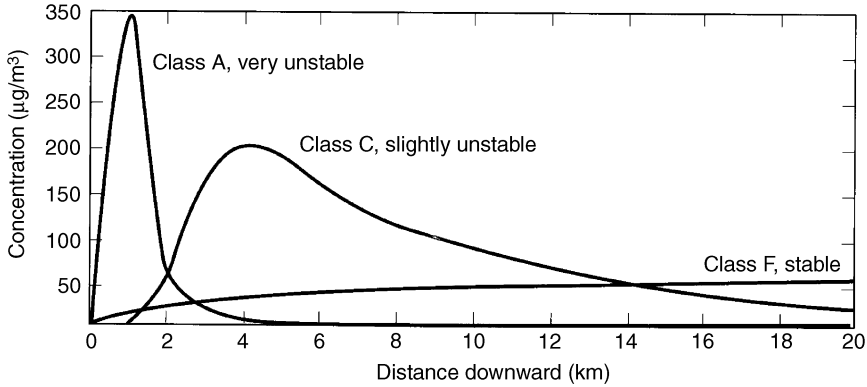

Figure 6.11 Variation of ground level concentration with distance downwind, under different atmospheric stabilities.
Source: Masters, G. M. (1998) *Environmental Engineering and Science*, Prentice Hall, New Jersey.

deviation with distance from the source for the different Pasquill stability categories. Note that the x scale runs from 100 m to 100 km – this dispersion methodology is designed for medium physical scales, neither small enough to be influenced by individual topographic features nor large enough to be controlled by synoptic windflows. Note also that σ_z, the vertical standard deviation, is much

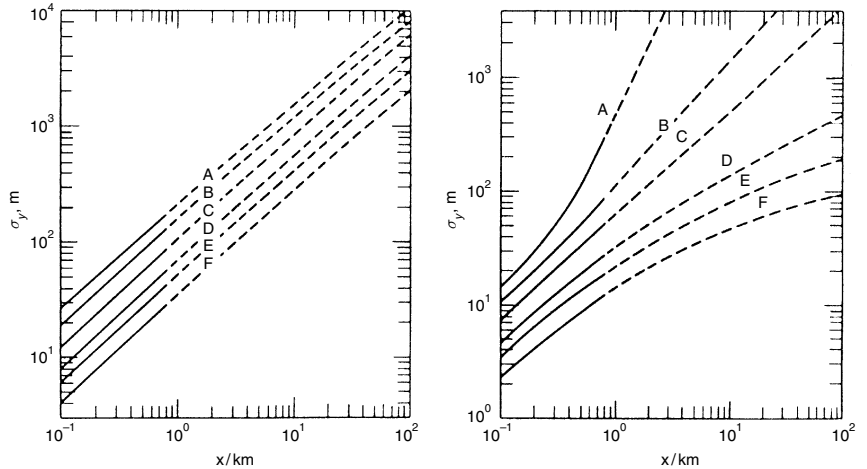

Figure 6.12 Variations of plume standard deviation in the *y* and *z* directions with distance x from the source. A, B, C, D, E and F are Pasquill stability categories.

Table 6.7 Equations for the variation of σ_y and σ_z with stability class

Pasquill category	σ_y/m	σ_z/m
Open-country		
A	$0.22x\ (1 + 0.0001x)^{-0.5}$	$0.20x$
B	$0.16x\ (1 + 0.0001x)^{-0.5}$	$0.12x$
C	$0.11x\ (1 + 0.0001x)^{-0.5}$	$0.08x\ (1 + 0.0002x)^{-0.5}$
D	$0.08x\ (1 + 0.0001x)^{-0.5}$	$0.06x\ (1 + 0.0015x)^{-0.5}$
E	$0.06x\ (1 + 0.0001x)^{-0.5}$	$0.03x\ (1 + 0.0003x)^{-1}$
F	$0.04x\ (1 + 0.0001x)^{-0.5}$	$0.016x\ (1 + 0.0003x)^{-1}$
Urban		
A–B	$0.32x\ (1 + 0.0004x)^{-0.5}$	$0.024x\ (1 + 0.001x)^{0.5}$
C	$0.22x\ (1 + 0.0004x)^{-0..5}$	$0.20x$
D	$0.16x\ (1 + 0.0004x)^{-0.5}$	$0.14x\ (1 + 0.0003x)^{-0.5}$
E–F	$0.11x\ (1 + 0.0004x)^{-0.5}$	$0.08x\ (1 + 0.0015x)^{-0.5}$

more influenced by stability than is σ_y, the horizontal standard deviation, owing to the influence of buoyancy forces.

Table 6.7 gives corresponding equations for open-country and urban conditions. The main difference is that the greater surface roughness in built-up areas generates greater turbulence.

6.3.8 Versions of the Gaussian equation

The full Gaussian equation (6.7) describes the concentration field everywhere in the free atmosphere due to a point source. More usually, we need to know the concentration at ground level, or from a ground level source, or directly downwind of the source. In these cases various simplifying assumptions can be made.

Ground-level concentration due to an elevated source, bounded by the ground surface

Set $z = 0$ everywhere in equation (6.7)

$$q(x, y, 0) = \frac{Q}{\pi \bar{u} \sigma_y \sigma_z} \exp - \left[\frac{y^2}{2\sigma_y^2} + \frac{H^2}{2\sigma_z^2} \right]$$

Ground-level concentration due to an elevated source, bounded by the ground surface, directly downwind of the source at ground level

Set $y = z = 0$ everywhere in equation (6.7).

$$q(x, 0, 0) = \frac{Q}{\pi \bar{u} \sigma_y \sigma_z} \exp \left[\frac{-H^2}{2\sigma_z^2} \right] \tag{6.10}$$

It can also be shown that the maximum downwind concentration, q_{max}, is given by

$$q_{max} = \frac{2Q}{\pi \bar{u} e H^2} \frac{\sigma_z}{\sigma_y} \tag{6.11}$$

at the distance x_{max} for which $\sigma_z = \frac{H}{\sqrt{2}}$.

In equation (6.11), $e = 2.71828$, the base of natural logarithms. First, use the known value of H to calculate σ_z, and read off this value on the vertical axis of Figure 6.12(b). Now move across to the curve corresponding to the known stability class, and read down to the horizontal axis to find x_{max}. Set this value on the x-axis of Figure 6.12(a), and read up to the same stability class and across to the y-axis. This gives the value of σ_y at x_{max}. Finally, use these values of σ_y and σ_z, together with Q, u and H, to find q_{max} from equation (6.11).

Note that the maximum ground-level concentration is inversely proportional to the square of the effective release height H, so that building taller chimneys is a very cost-effective method of reducing ground-level pollution.

Ground-level concentration due to a ground level source, directly downwind of the source (e.g. bonfire)

Set $y = z = H = 0$

Hence

$$q(x, 0, 0) = \frac{Q}{\pi \bar{u} \sigma_y \sigma_z} \tag{6.12}$$

Line source. When a continuous series of point sources moves along a line, as vehicles do along a road, they are equivalent to a continuous line source. If the x-axis is perpendicular to the road, then there is no variation of concentration in the y direction, and we have

$$q(x, z) = \sqrt{\frac{2}{\pi}} \frac{Q}{\bar{u} \sigma_z} \exp\left[\frac{-z^2}{2\sigma_z^2}\right] \tag{6.13}$$

where Q now has units of kg m^{-1} s^{-1}.

6.4 DISPERSION THEORY IN PRACTICE

Do not be misled into thinking that the neat-looking equations given above provide us with an infallible method of predicting dispersion – they fall well short of this ideal. Many field measurement programmes have been undertaken to validate both the plume rise and dispersion equations. A favourite method for evaluating plume dispersion is to release sulphur hexafluoride (SF_6) into the flue gases where they

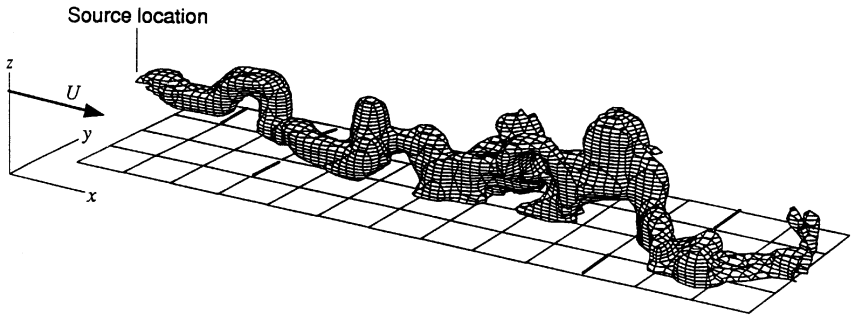

Figure 6.13 A modelled surface of constant concentration downwind of a continuous release.
Source: Henn, D. S. and Sykes, R. I. (1992) 'Large-eddy simulation of dispersion in the convective boundary layer', *Atmospheric Environment* 26A(17): 3145–3159.

enter the stack. SF_6 is a passive conservative tracer – it is very stable and there is no ambient background, so one can be sure that the concentration measured in the ambient air was emitted from the source under investigation and not from somewhere else altogether. Alternatively, the sulphur dioxide emissions from major commercial sources such as power stations have been monitored. The underlying problem in validation is the large spatial and temporal variability of the plume concentrations caused by the random nature of atmospheric turbulence. This is graphically illustrated by Figure 6.13, which is a computer simulation of plume geometry – the wiggly tube represents a snapshot of a surface of constant concentration. Dispersion theory must predict the average concentration at a point in space due to the highly variable exposure of that point to this fluctuating plume.

6.4.1 Worked example of Gaussian dispersion

We will apply the concepts that have been described above to predict the downwind ground-level concentration of sulphur dioxide that will be produced from a chimney of known height. We are given the following information:

Source characteristics
Height 100 m
Internal radius 5 m
Exit speed 20 m s^{-1}
Exit temperature 80 °C = 353 K
Coal burn = 3000 t day^{-1}: S content = 1.4%

Environmental conditions
Windspeed at 10 m = 8 m s^{-1}

Weather – cloudy
Air temperature at stack height = 10 °C = 283 K

Receptor location
6000 m downwind of the source, at ground level on flat terrain.

The data given above have been invented for this example, but are representative of a medium-sized coal-fired facility. The same Gaussian equations can be applied to a wide range of possible source configurations and weather conditions.

Step 1. Find the stability category

Use Table 6.3 to find the stability from the environmental conditions. Because it is windy and cloudy, we have Category D.

Step 2. Calculate σ_y and σ_z

Now go to Table 6.7. In open country, with stability category D and $x = 6000$ m, we have

$$\sigma_y = 0.08 \times 6000\,(1 + 0.0001 \times 6000)^{-0.5} = 379 \text{ m; and}$$
$$\sigma_z = 0.06 \times 6000\,(1 + 0.0015 \times 6000)^{-0.5} = 113 \text{ m.}$$

Step 3. Calculate the windspeed at the release height

Use Equation (6.1) to find the windspeed at 100 m. From Table 6.1 for Category D, $p = 0.15$. Hence $u(100) = 8(100/10)^{0.15} = 11.3$ m s^{-1}

Step 4. Calculate the plume rise and effective release height

From

$$F_b = w_0 R_0^2 \frac{g}{T_{p0}} (T_{p0} - T_{a0}),$$

the buoyancy flux $F_b = 20 \times 5^2 \times 9.81 \times (353–283)/353 = 973$ m^4 s^{-3}. Following Section 3.3.1, with Category D and $F_b > 55$, we use equation (6.6) to find the plume rise dh. Hence $dh = 39 \times 973^{0.6}/11.3 = 214$ m and $H = 100 + 214 = 314$ m.

Step 5. Calculate the SO_2 release rate

Coal burn = 3000 t day^{-1}, S content = 1.4%
Sulphur emission = $0.014 \times 3000/(24 \times 60 \times 60)$ t s^{-1}
$= 4.86 \times 10^{-4}$ t s^{-1} $= 4.86 \times 10^2$ g S s^{-1}
Sulphur dioxide emission = 2 × S emission (because the molecular weight of SO_2 is twice that of S) = 9.72×10^2 g s^{-1}.

Step 6. Solve the dispersion equation

For ground-level concentration on the plume centre-line, use equation (6.10).

$$q(x, 0, 0) = \frac{Q}{\pi \bar{u} \sigma_y \sigma_z} \exp\left[\frac{-H^2}{2\sigma_z^2}\right]$$

with $Q = 9.72 \times 10^2$ g s^{-1}, $u = 11.3$ m s^{-1}, $\sigma_y = 379$ m, $\sigma_z = 113$ m and $H = 314$ m.

Hence

$$q(6000, 0, 0) = \frac{9.72 \times 10^2}{\pi \times 11.3 \times 379 \times 113} \exp\left[-\frac{314^2}{2 \times 113^2}\right]$$
$$= (6.39 \times 10^{-4}) \times 0.021$$
$$= 13.4 \times 10^{-6}\,\mathrm{g\,m^{-3}} = 13.4\,\mu\mathrm{g m^{-3}} \text{ (about 5 ppb)}$$

6.4.2 Predictions for planning purposes

When a new industrial development involving pollutant emissions is proposed, calculation of pollutant concentrations can become an important component of the environmental impact assessment. Long-term exposures due to a point source are determined by accumulating average values for the 8760 hourly means of wind direction, windspeed, atmospheric stability and other environmental variables, and then running the dispersion model for each hour. The most important factor is the wind rose – the proportion of the time for which the wind blows from each direction (Figure 6.14).

Commonly, the 360° of the compass will be divided up into 16 sectors of 22.5° or 32 sectors of 11.25°, and the pollutant concentration determined while the wind is blowing from that sector. The resulting angular distribution is then called the pollutant rose. Since the statistical distribution of the concentrations follows

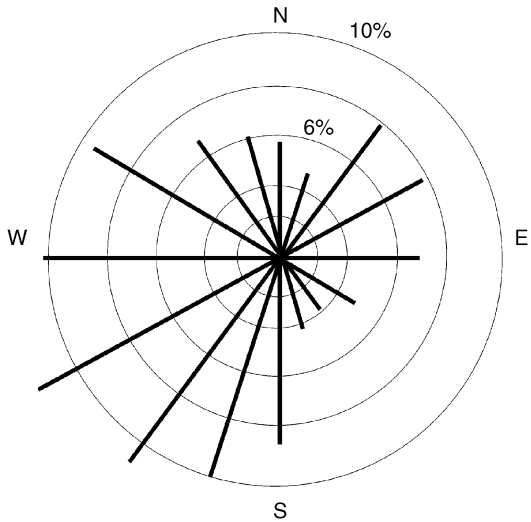

Figure 6.14 A typical windrose. The length of the bar shows the proportion of the time for which the wind was blowing from the sector centred on that direction.

a log-normal pattern, the correct description of concentrations is in terms of the median (the value exceeded for half the time, or 4380 h), together with the 10% (876 h) and 1% (88 h) exceedances. Very often organisms, including people, respond to the highest values that occur for the shortest periods, so that this knowledge of statistical distribution is important for predicting effects. Measurement of the pollutant rose also suggests attribution of the concentrations to a particular source. In many areas of the UK, winds come most often from the south-west to west sector and from the north-east, and this is reflected in the geographical distribution of concentrations around a source.

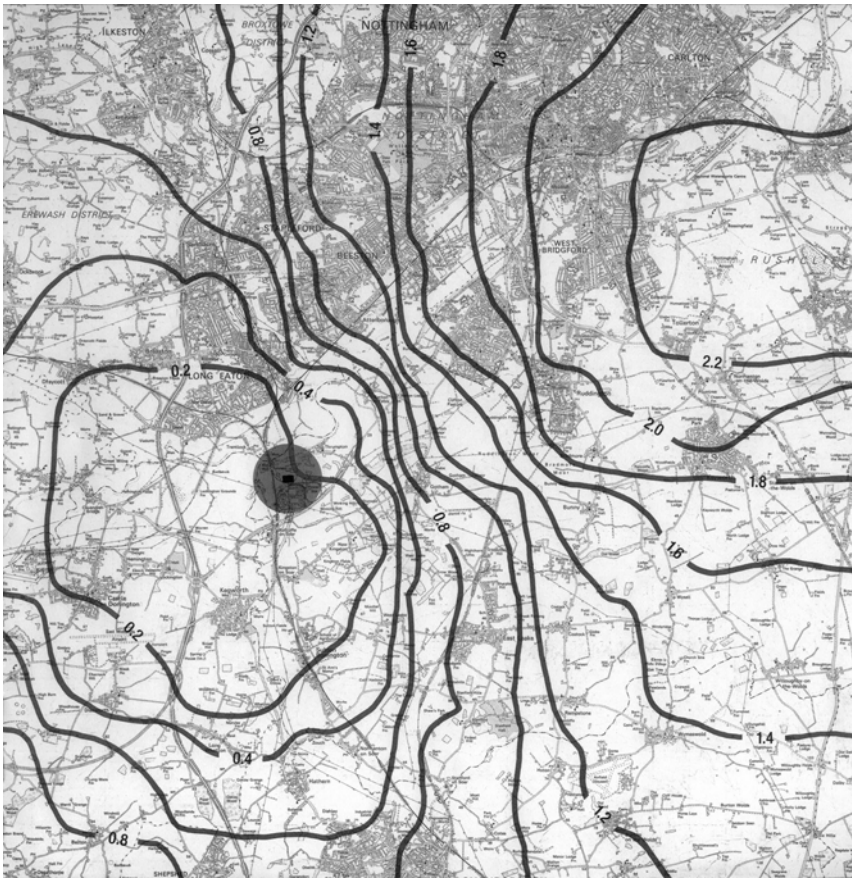

Figure 6.15 Annual average contours of ground-level sulphur dioxide concentration predicted around the PowerGen power station at Ratcliffe-on-Soar. The power station is the rectangle within the dark circle. The urban area to the north-east is Nottingham. The contours are at intervals of 0.2 μg m^{-3}.
Source: PowerGen *Environment Statement for the Proposed Flue Gas Desulphurisation Plant, Ratcliffe-on-Soar Power Station*, PowerGen, UK.

Figure 6.15 shows an example of calculations made at the planning stage of a new Flue Gas Desulphurisation plant being designed for the PowerGen power station at Ratcliffe-on-Soar, Nottinghamshire, UK. Average dispersion conditions were calculated for each hour of the year, and a Gaussian model used to calculate the pollution contours for that hour. All the individual hours were then combined to give the annual average contours shown. The modelled contours of sulphur dioxide concentration show one peak to the north-east due to winds from the south-west, and a second, much lower, peak to the south-west due to the much lower proportion of wind from the north-east. Other, less obvious, factors also influence concentrations; for example, windspeed is correlated with wind direction, and higher windspeeds will usually reduce concentrations.

There may be complications in matching the predicted concentrations to guidelines and limit values. For example, the UK air quality standard for SO_2 specifies a 15-min mean of 266 $\mu g\ m^{-3}$ as the 99.9th percentile (equivalent to no more than 35 exceedances per year), whereas the Chimney Heights Memorandum (which must be used by Local Authorities to calculate stack heights for planning purposes) specifies 452 $\mu g\ m^{-3}$ as a 3-min average. In such cases, empirical factors derived from more complete data sets can be used to convert. For example, the factor 1.34 is recommended to convert the 99.9th percentile 15-min mean from short stacks to the 99.9th percentile 1-h mean. Unfortunately the factor itself varies with parameters such as stack height, adding another level of uncertainty to the predictions.

6.4.3 Effects of topography

The simplest dispersion theory deals with a source situated in the middle of a flat plain. Although such sources do exist, most landscapes involve hills of some sort, and for some landscapes the hills seriously affect dispersion.

Valleys tend to deviate and concentrate the wind flow, so that the average windspeed is higher than, and the wind blows along the valley for a higher proportion of the time than, would be expected in the open. There will also be thermal effects due to differential heating of the valley sides. For example, the north side of an east-west oriented valley will receive stronger solar radiation during the day than the south side. This asymmetry will generate a convective circulation which involves air rising up the relatively warm northern slope and descending down the relatively cool southern slope. At night, cool air may accumulate in the valley floor, producing a stable temperature inversion in which pollutants emitted from activities on the valley floor (which is where towns, roads and factories tend to be located) will accumulate.

The actual flow pattern of air over non-uniform terrain is not easy to predict or measure. For an isolated obstacle, the upwind streamlines are gradually compressed as the flow approaches the obstacle. At some point near the obstacle, the flow separates, with a turbulent and possibly recirculating region in the downstream wake where the wind direction will be opposite to the initial direction. At some further distance downstream the flows converge again. The wake region

must be allowed for in pollutant release calculations; if an emission is released into such a recirculation zone, it can build up to much higher concentrations than simple dispersion theory would indicate. Air flow over hilly terrain will involve a mixture of processes. In smoother areas, the streamlines will follow the contours. In rougher areas there may be flow separation and turbulent wake formation under some combinations of wind direction and speed but not under others.

6.4.4 Effects of buildings

It would be unusual for any emission to be released from an isolated chimney, standing alone in the middle of a flat plain. More often, the chimney will be part of a complex of other buildings which disturb the flow in the boundary layer and change the dispersion of the chimney gases. The flow patterns are very complex, and only the main features will be indicated here. Furthermore, the predictions are part-theoretical, part empirical and part based on wind-tunnel studies which often do not reliably predict full-scale field results. The main features of the disturbed flow for air impinging directly onto the upwind face of a cuboidal building are seen in Figure 6.16.

- a stagnation point (SP) where streamlines impinge on the upwind face
- a recirculating flow region, separated from the main flow, immediately downwind of the downstream face. This recirculation may separate from the top edge of the upwind face, or it may attach to the roof and separate from the top edge of the downstream face. Concentrations are assumed to be uniform in this well-mixed region
- a downstream wake where the turbulence is enhanced and the average flow vector is down toward the ground
- a long trail of more structured (i.e. less randomised) vortices downwind.

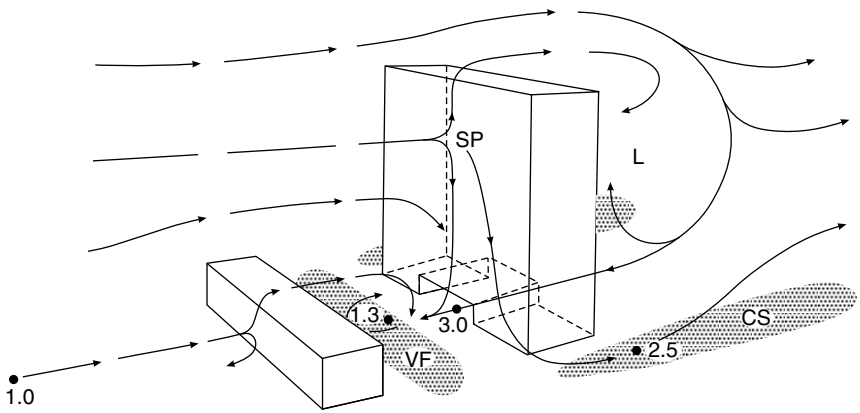

Figure 6.16 Idealised flow pattern round a cuboidal building. Values are relative wind speeds; SP = stagnation point; CS = corner stream; VF = vortex flow; L = lee eddy.

The effects of these disturbances on the dispersion of emissions from the building, or from nearby sources, depend sensitively on the exact position and characteristics of the source. For example, a weak (in the jet sense) source close to the roof may be entrained into the recirculation, and thence into the wake, or it may mix into the wake, or it may avoid both and mix into the undisturbed flow. Variable proportions of the plume may also experience these histories. If a roof level emission does not escape the recirculation, then its effective emission height will be zero. This can clearly have serious consequences for downwind pollution concentrations.

6.4.5 Recent developments

The Pasquill categorisation scheme was the first method to be widely adopted for relating plume standard deviation to atmospheric conditions, and has become the most generally used. Although it has proved its worth in many trials, it has certainly got important deficiencies. The method works best under stable and neutral conditions, but tends to fail under the more fluctuating conditions typical of an unstable atmosphere. In order to improve the predictions, changes have been made to the model. First, the values of σ_y and σ_z can be derived from fundamental characteristics of turbulence. If we measure the lateral and vertical components of windspeed (v and w respectively), we find that there is a normal distribution of speeds above and below the mean. The widths of these distributions can be characterised by their standard deviations, σ_v and σ_w, which can then be related in turn to the standard deviation of the concentration.

The Gaussian model is in widespread use because of its comparative simplicity, but it should be clear by now that it can only offer rather coarse predictions of dispersion in practice. More powerful models have been developed based on more rigorous turbulence theory. Although a detailed treatment is beyond the scope of this book, we can see the potential improvements. Figure 6.17 gives an example of how an SF_6 release experiment was used to test the differences in prediction performance of two dispersion models used in the US. In each graph, the measured 1-h average concentration c_o is plotted against the concentration predicted by the particular model, c_p. The 'pdf' model (Figure 6.17(a)) is based on the probability distribution function describing the relative abundance of convective updraughts and downdraughts in the advecting plume, while the CRSTER model (Figure 6.17(b)) is a conventional Gaussian dispersion model as described above. In this instance the pdf model clearly offered improved prediction power over the standard Gaussian. In particular, the concentration c_p predicted by the Gaussian model was zero on a large number of occasions when a concentration was actually observed (the column of points up the y axis of Figure 6.17(b)). The correlation coefficient of the pdf model was substantially higher than that of the Gaussian ($r^2 = 0.34$, 0.02 respectively).

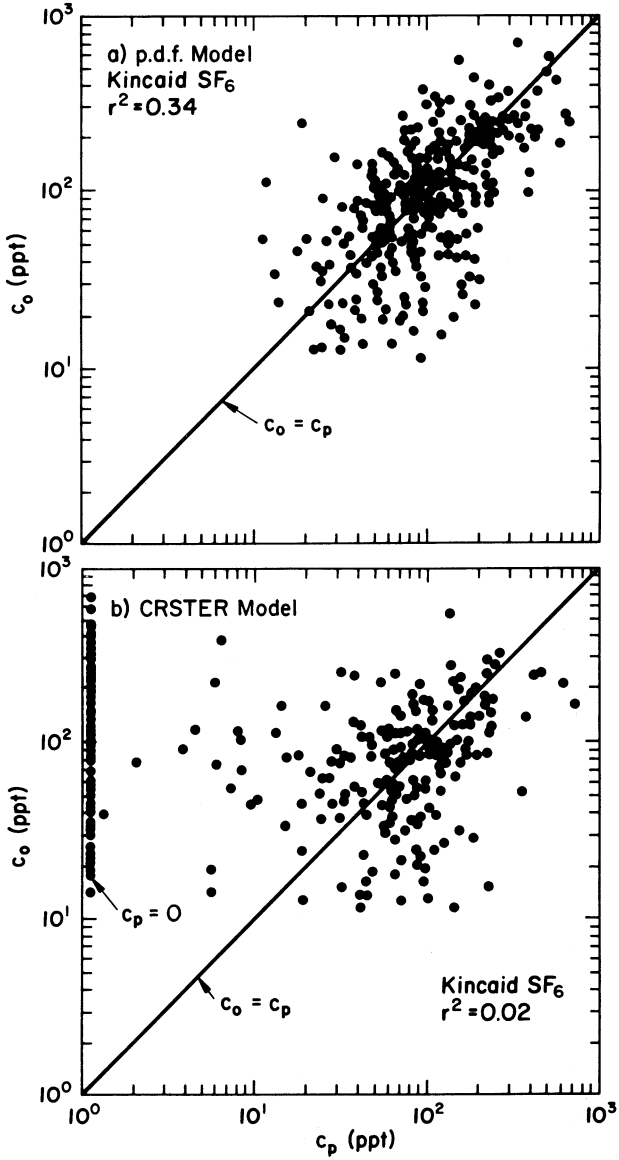

Figure 6.17 Comparisons of measured ground level concentrations with those predicted by: (a) the 'pdf' model; and (b) a standard Gaussian model. Source: Weil, J. C., Sykes, R. I. and Venkatram, A. (1992) 'Evaluating air-quality models: review and outlook', *Journal of Applied Meteorology* 31(10): 1121–1145.

6.5 DISPERSION OF VEHICLE EMISSIONS

In Chapter 2, we discussed the complicated set of procedures that has to be undertaken in order to compile an estimate of vehicle emissions. After these source strengths (in g m^{-1} s^{-1}, for example) have been calculated, ambient concentrations can be found from dispersion theory. Away from built-up areas, for motorways, main roads and other roads in the open, the Gaussian method described above can be used. There are many implementations of the method in common use; for example, a model called CALINE was developed in California, and has evolved into CALINE4. The basic principles are quite straightforward. An urban network of roads is divided into links, where each link is a straight length of road having known emission characteristics. That link is treated as a line source for the calculation of concentrations at receptors (the points at which a concentration estimate is required). The total concentration at the receptor is the sum of the contributions due to all the individual links, plus any background concentration due to the unmapped parts of the area. There are certain features of the dispersion that are not catered for in the simple Gaussian method. For example, the effective source is regarded as the roadway itself, after initial dilution of the exhaust gases by mechanical (wake) and thermal (due to waste vehicle heat) turbulence. These effects are used to modify the dispersion parameters such as stability class.

In built-up urban areas, simple Gaussian dispersion theory does not apply – the sources are often at the bottom of 'street canyons' which reduce windspeeds below the ambient level, especially when the wind direction is almost perpendicular to that of the road. Under those conditions, a recirculating vortex can keep emissions confined within the canyon, so that road-level concentrations build up to several times the values they would have in the open. Several methods of analysis have been developed for this situation. One example is the Canyon Plume Box (CPB) model originally developed for the German EPA and subsequently refined by the US Federal Highway Administration. CPB models the vehicle-induced initial turbulence, plume transport and dispersion (Gaussian) on the lee side of the canyon, advective and turbulent exchange at the top of the canyon, pollutant recirculation, and clean air injection on the downwind side of the canyon. Allowance can also be made for the effects of canyon porosity – i.e. gaps in the canyon wall due to intersections, missing buildings or other irregularities.

The UK Meteorological Office has produced a simple model called Assessing the Environment of Locations In Urban Streets (AEOLIUS) to screen for worst case conditions in urban areas, on the assumption that the highest concentrations are produced by only two conditions – wind direction parallel or perpendicular to the road. As a result of this simplification they were able to reduce the complex computer modelling to a paper nomogram. First an uncorrected concentration is calculated for the prevailing windspeed and unit emissions. This is then multiplied by four correction factors estimated graphically from values for canyon height and width, and traffic flow and speed.

Modelling pollutant concentrations due to vehicles involves calculation of source strengths for a series of roadlinks, then dispersion in an urban area that usually consists of a mixture of open and canyon environments. At Nottingham, we developed a general-purpose suite of vehicle emission and dispersion models, called SBLINE. SBLINE uses a very detailed evaluation of emissions based on local measurements (if available) or default estimates. It is crucial to estimate this source strength as accurately as possible for the particular circumstances, making due provision for the components of the vehicle fleet (types of vehicle, year of legislation under which manufactured, or operating mode). If a receptor lies in a canyon, then CPB is used to find the contribution due to sources on that link, and NOTLINE for the contributions due to all other links. If the receptor lies on open ground, then NOTLINE is used throughout. This model has been validated against measured carbon monoxide concentrations in Leicester, UK. A specific part of Leicester was chosen within the City's Urban Traffic Control scheme, so that information on traffic flow was available. Three continuous carbon monoxide analysers were sited on London Road. Detailed surveys were carried out to build up profiles of traffic flows, vehicle age structure (from number plates), vehicle types, and periods spent in different operational modes. These data were input to SBLINE to predict the CO concentrations at the three receptor sites. Figure 6.18 shows the capability of the model in predicting both the average level and temporal variations in CO.

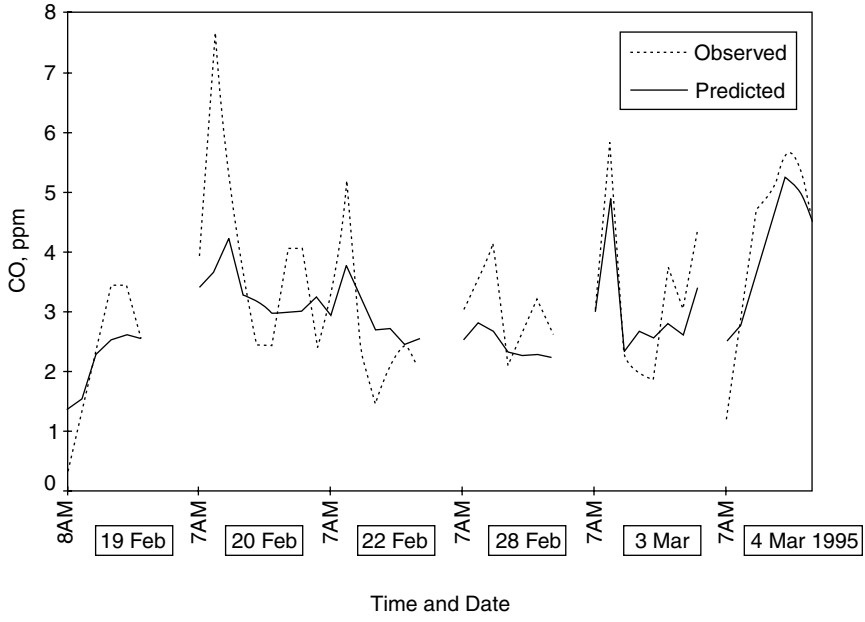

Figure 6.18 Comparison of the measured and modelled CO concentrations over the period 19 February–4 March 1995.
Source: A. Namdeo. (Pers. Com.)

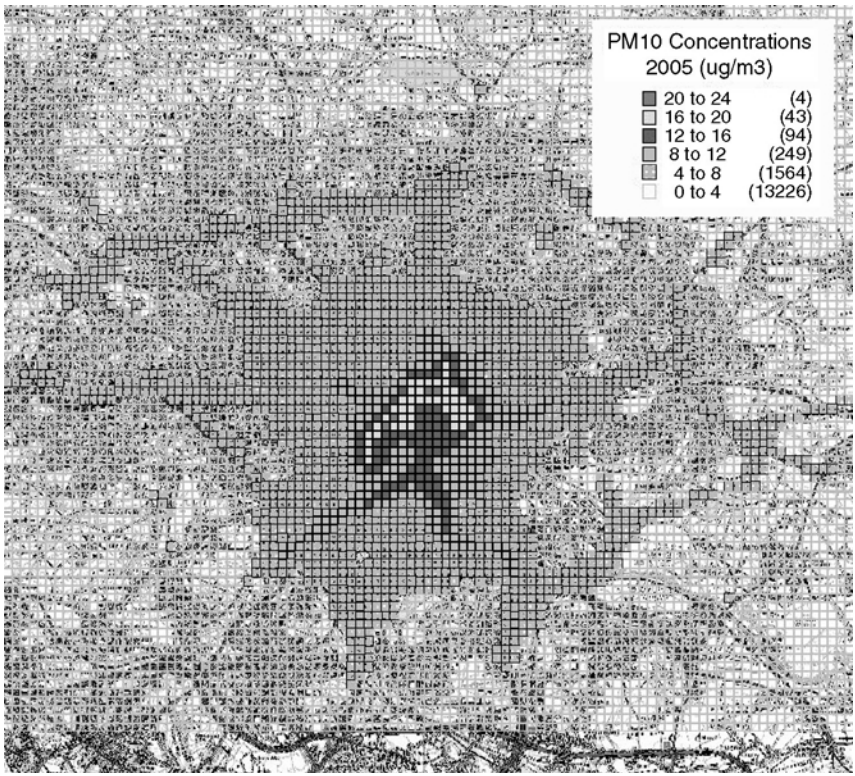

Figure 6.19 Predicted PM_{10} concentrations around Leeds in 2005. Source: A. Namdeo. (Pers. Com.)

This approach can be developed into a model of a whole urban area, such as that shown in Figure 6.19 for Leeds, UK. Having made predictions for 2005 of the traffic flows on the network of roads around Leeds, and allowing for factors such as the change in vehicle emission control by then, the variation of PM_{10} concentrations across the city has been calculated. This kind of output can then be used to improve urban planning and meet air quality guidelines.

6.6 RECEPTOR MODELS

Receptor models are used to estimate the contribution of different sources to the concentration at a location (the receptor) using statistical evaluation of the data collected at that receptor. This process is called source attribution or source apportionment. Receptor models have been used most intensively for the attribution of sources to explain particle concentrations, because the distinctive

chemical fingerprints of particles enable them to be identified with specific emissions. In some ways the process is the reverse of dispersion modelling, because the source is worked out from the concentration, rather than *vice versa*. The first step is to collect a large data set of concentration measurements at the receptor, using as comprehensive analysis as possible. Typically elemental, organic and gaseous concentrations would be measured, as well as particle concentration and possibly size distributions. Intensive and sophisticated analytical methods would often be used, such as X-ray fluorescence, ICP-MS, PIXE and neutron activation analysis. Certain elemental tracers may be used to identify sources, such as lead for petrol, but in that case the link needs to be unambiguous. Hydrocarbons such as ethane and propane may be used as tracers for exhaust or petrol storage tank emissions, PAH for wood combustion and diesel smoke, toluene for solvents. In chemical mass balance methods, data on chemical composition of the ambient measurements is related to that of known emissions. It is assumed that the elements or compounds are not reactive in the atmosphere. Clearly the chemical and physical characteristics of the measured pollutants emitted from different potential sources must be different, and those characteristics must be preserved during transit through the atmosphere to the receptor. By using more powerful statistical methods, such as principal component analysis (PCA) with multiple linear regression, the sample properties alone can be used to work out the number of source categories, the chemical composition of their emissions and their relative contributions to the measured concentrations. This is necessary if some sources have not been identified or if their emission characteristics are poorly defined – as with roads.

6.6.1 Chemical mass balance models

Chemical mass balance was the first receptor modelling method developed for source attribution. It uses two data sets: (1) the chemical composition of the atmospheric aerosol at a measurement site; and (2) the chemical composition of the aerosol emitted from the principal sources in the region. The material collected, for example on a high-volume filter paper, is composed of contributions from various sources

$$\rho = \sum_{j}^{p} m_j \, (j = 1, 2, \ldots p)$$

where ρ is the local aerosol mass concentration, m_j is the contribution from source j, and there are p sources altogether. In practice, there may be some discrete individual sources if large local ones exist, and other smaller sources will be lumped and treated collectively as domestic, vehicular etc. It is also normally assumed that the overall chemical balance of the sources is the same as that at the receptor – i.e. that there have been no changes due to selective deposition or gas/particle conversion.

The concentration ρ_i of the ith chemical component in the aerosol sample is related to the source contributions by

$$\rho_i = \sum_j^p c_{ij} m_j (i = 1, 2, \ldots n)$$

where c_{ij}, which is the mass fraction of component i in m_j, is the source concentration matrix, and there are n chemical components. The main task is to invert this equation to give the source contributions m_j. This could be done by varying the source contributions to minimise the weighted mean square deviations. The method has been applied to a wide variety of source attribution problems, from single point sources to complex urban and regional airsheds and Arctic air quality.

6.7 BOX MODELS

Box models are the simplest ones in use. As the name implies, the principle is to identify an area of the ground, usually rectangular, as the lower face of a cuboid which extends upward into the atmosphere. A budget is then made on the box over a specified timestep, for the pollutant(s) of interest. This budget will involve the initial contents of the box due to the prevailing pollutant concentration, emissions into the box from sources, deposition from the box to surfaces, additions/losses to/from the box due to wind and concentration gradients, and gains/losses due to chemical reactions. At the end of the timestep, a new average concentration within the box is calculated, and the process is repeated to track temporal variation of the pollutant concentration. Spatial variability is calculated by having a grid of adjacent boxes of appropriate size, and vertical variations by extending the boxes upwards using the same principles.

6.8 STATISTICAL MODELS

Statistical models do not involve emissions at all. Data on concentrations at a location are collected, together with data on local factors that might affect those concentrations. Such factors might include wind direction and speed, solar radiation, air temperature, time of day, day of the week, season. Statistical correlations are made to suggest what proportion of the variability of the concentration about the mean value is due to each of the factors. Then if a value for each of the factors is known, an estimate can be made of the likely concentration. Because it is based on historical data sets, the prediction assumes that the influence of the factors on concentration will be the same in the future. This is likely to be true on a few-day timescale; of course, each new day's data set may be input to the model so that any gradual changes in the effects of the different factors are incorporated.

FURTHER READING

Arya, S. P. (1999) *Air Pollution Meteorology and Dispersion*, Oxford University Press, New York.

Lyons, T. J. and Scott, W. D. (1990) *Principles of Air Pollution Meteorology*, Belhaven Press, London, UK.

Pasquill, F. and Smith, F. B. (1983) *Atmospheric Diffusion*, Ellis Horwood, Chichester, UK.

Turner, D. B. (1994) *Workbook of Atmospheric Dispersion Estimates*, CRC Press, Boca Raton, Florida.

UK Department of the Environment, Transport and the Regions (1998) *Selection and Use of Dispersion Models*, Stationery Office, London.